AGU PUBLICATIONS

JGR

Journal of Geophysical Research: Biogeosciences

RESEARCH ARTICLE
10.1002/2015JG003091

Key Points:
- Rain pulses promote net CO_2 emissions over the dry season
- Net CO_2 uptake is only triggered by large rainfall events
- Soil respiration increases after rain pulses regardless of their magnitude

Correspondence to:
A. López-Ballesteros,
alballesteros@eeza.csic.es

Citation:
López-Ballesteros, A., P. Serrano-Ortiz, E. P. Sánchez-Cañete, C. Oyonarte, A. S. Kowalski, Ó. Pérez-Priego, and F. Domingo (2016), Enhancement of the net CO_2 release of a semiarid grassland in SE Spain by rain pulses, *J. Geophys. Res. Biogeosci.*, *121*, 52–66, doi:10.1002/2015JG003091.

Received 9 JUN 2015
Accepted 3 DEC 2015
Accepted article online 11 DEC 2015
Published online 9 JAN 2016

Enhancement of the net CO_2 release of a semiarid grassland in SE Spain by rain pulses

Ana López-Ballesteros[1,2], Penélope Serrano-Ortiz[2,3], Enrique P. Sánchez-Cañete[2,4], Cecilio Oyonarte[5,6], Andrew S. Kowalski[2,7], Óscar Pérez-Priego[8], and Francisco Domingo[1]

[1]Departamento de Desertificación y Geo-ecología, Estación Experimental de Zonas Áridas (CSIC), Almería, Spain, [2]Centro Andaluz de Medio Ambiente (IISTA), Granada, Spain, [3]Departamento de Ecología, Universidad de Granada, Granada, Spain, [4]Biosphere 2, University of Arizona, Tucson, Arizona, USA, [5]Departamento de Agronomía, Universidad de Almería, Almería, Spain, [6]Centro Andaluz de Evaluación y Seguimiento del Cambio Global, Almería, Spain, [7]Departamento de Física Aplicada, Universidad de Granada, Granada, Spain, [8]Max Planck Institute for Biogeochemistry, Jena, Germany

Abstract Occasional rain events occur over the dry season in semiarid ecosystems and cause immediate, large increases in the net CO_2 efflux which gradually decrease over a few days following the rain event. In a semiarid grassland located in SE Spain, these precipitation pulses represent only 7% of dry season length but provoked approximately 40% of the carbon emitted during the dry seasons over 2009–2013. We performed a manipulation experiment to decompose the net ecosystem pulse response into its biological processes in order to quantify how much of a role photosynthesis and aboveground respiration play compared to soil respiration. Experimental results showed that while soil respiration was the dominant component of the net CO_2 flux (net ecosystem CO_2 exchange, NEE) over the irrigation day and the day after (80% of NEE), plant photosynthesis remained inactive until 2 days after the pulse, when it appeared to become as prevalent as soil respiration (approximately 40% of NEE). Additionally, aboveground respiration was generally secondary to soil respiration over the whole experiment. However, statistical results showed that aboveground carbon exchange was not significantly affected by the rain pulse, with soil respiration being the only component significantly affected by the rain pulse.

1. Introduction

Arid and semiarid ecosystems comprise nearly a third of the total land surface [*Okin*, 2001; *Schlesinger*, 1990] and play a pivotal role in the global carbon (C) balance [*Ahlström et al*., 2015; *Metcalfe*, 2014; *Poulter et al*., 2014], owing to their dynamic behavior modulated by precipitation events. In this regard, rain pulses are common and stochastic water inputs that strongly determine arid land structure and function [*Ehleringer et al*., 1999; *Lázaro et al*., 2001; *Noy-Meir*, 1973], especially after an extended period of hydric stress. In Mediterranean regions, occasional summer and early autumn storms fit this concept due to their brevity and unpredictable nature [*Cleverly et al*., 2013; *Lázaro et al*., 2001] and even can be recognized as a transition phase between dry and growing seasons.

Some studies have examined regional-scale rain pulse responses using satellite imagery and climatic data. For example, *Li et al*. [2013] found correlations between the magnitude of rain events and the photosynthetic activity increase in two different arid ecosystems. Conversely, *Zhang et al*. [2013] concluded that the combination of heavy rainfalls with dry periods led to a reduction in primary production. Measurements of CO_2 exchanges at the ecosystem scale also highlighted an enhancement of C release triggered by rain pulses under dry conditions [*Jenerette et al*., 2008; *Ross et al*., 2012; *Williams et al*., 2009]. However, deeper knowledge is needed in order to understand the mechanisms by which rain pulses affect the biological processes that compose the overall net ecosystem response.

In this sense, most research has focused on either soil processes [*Fan et al*., 2012; *Leon et al*., 2014; *Sponseller*, 2007; *Unger et al*., 2010] or plant physiological responses [*Balaguer et al*., 2002; *Padilla et al*., 2015; *Pugnaire et al*., 1996]. Accordingly, few studies have simultaneously and separately tracked the effect of rain pulses on the overall components of the ecosystem C balance in order to disentangle all the processes composing the total effect on net ecosystem CO_2 exchange (NEE) [*Huxman et al*., 2004a; *Unger et al*., 2012].

In this study, we have assessed the relevance of rain pulses over the dry season C balance of a semiarid grassland located in SE Spain through the analysis of eddy covariance (EC) data from 2009 to 2013. In addition,

given the complexity of C dynamics in these regions, we simulated a realistic rain pulse in order to delve into the short-term response of the distinct biological processes that compose the overall rewetting effect on NEE, monitoring aboveground and belowground C exchanges. For this purpose, we have integrated novel methodologies, such as transient-state canopy chambers, soil chambers, and subsoil continuous CO_2 sensors, to directly measure aboveground net primary productivity (ANPP), soil respiration (R_{soil}), aboveground respiration ($R_{aboveground}$), and plot-scale NEE (i.e., NEE_{plot}). We hypothesize that rain pulses during the dry season provoke a relevant net C release by enhancing soil respiration processes, commonly known as the Birch effect [*Birch*, 1959; *Carbone et al*., 2011; *Huxman et al*., 2004a; *Jarvis et al*., 2007; *Leon et al*., 2014; *Sponseller*, 2007; *Thomey et al*., 2011; *Unger et al*., 2010; *Wohlfahrt et al*., 2008]. Furthermore, since *Balaguer et al*. [2002] stated that the relevant species (*Machrocloa* sp.) has the ability to respond to punctual, infrequent, and random rain pulses, we expect activation of plant photosynthesis following rain events, regardless of pulse magnitude [*Lázaro et al*., 2001; *Sala and Lauenroth*, 1985], although this C assimilation may be offset or even exceeded by soil respiratory emissions. Accordingly, our objectives are as follows: (i) to quantify the contribution of rain pulse events to dry season NEE in this semiarid grassland, (ii) to detect differing NEE responses depending on the magnitude of rain pulses, and (iii) to determine if soil respiration, as well as plant photosynthesis (i.e., belowground and aboveground processes, respectively), activates following the rain events.

2. Material and Methods

2.1. Experimental Site Description

This study was carried out at the experimental site of Balsa Blanca (N36°56′26.0″, W2°01′58.8″), an alpha grassland located in the Cabo de Gata-Níjar Natural Park (Almería, Spain), at an altitude of 208 m above sea level and situated 6.3 km from the Mediterranean Sea. The climate is dry subtropical semiarid, with a mean annual temperature of 18°C and mean annual precipitation of approximately 220 mm. The growing (December–April) and nongrowing season mean temperature and precipitation are 13°C and 21°C and 145 mm and 114 mm, respectively, for the studied period. In this region, climatic conditions change between seasons, and most precipitation occurs during late autumn and winter; summer is the dry season with high temperatures and incident radiation. Prevailing soils, classified as Calcaric Lithic Leptosol [*World Reference Base for Soil Resources*, 2006], are thin (10 cm on average), alkaline (pH above 8), and include petrocalcic horizons [*Weijermars*, 1991]. Texture is sandy loam with sand (61%), silt (23%), and clay (16%) with a bulk density of 1.25 g cm^{-3}. Ground cover consists of bare soil, gravel and rock (49%), and vegetation (51%).

Although there are other species such as *Chamaerops humilis*, *Rhamnus lycoides*, and *Pistacia lentiscus*, the dominant species is *Machrocloa tenacissima* (57% of plant cover). This perennial tussock grass is very well adapted to semiarid and arid conditions owing to its shallow root system and physiological tolerance and avoidance strategies against hydric stress [*Haase et al*., 1999; *Pugnaire et al*., 1996]. *Machrocloa* sp. can be found in vast territories in Northwest Africa and the Iberian Peninsula [*Le Houérou*, 1986; *Rejos*, 2000], where it usually shows patchy distribution resulting in unequal availability of nutrients and water resources in drylands, which corresponds to the well-documented "islands of fertility" [*Charley and West*, 1975; *Cross and Schlesinger*, 1999; *Maestre et al*., 2007]. At our experimental site, the growing season begins in late autumn and ends in early spring, when the temperature starts to rise and water resources have not yet become scarce [*Serrano-Ortiz et al*., 2014]. More detailed site information is given by *Rey et al*. [2012].

2.2. Meteorological and Eddy Covariance Measurements and Data Processing

In this study we used meteorological and flux data from 2009 to 2013, acquired by an eddy covariance (EC) tower and complementary sensors (Table 1) installed in Balsa Blanca (site code "Es-Agu" of the European Database Cluster, http://www.europe-fluxdata.eu/). The CO_2, water vapor, and sensible heat fluxes were calculated from raw data acquired at 10 Hz and processed with EddyPro 5.1.1 software (Li-Cor, Inc., USA). Processing steps included spike removal, double axis rotation, correction for sensor separation, spectral corrections for high- and low-frequency ranges [*Moncrieff et al*., 2005, 1997], Reynolds averaging, and correction for density fluctuations [*Webb et al*., 1980]. Half-hourly averaged fluxes were rejected if missing raw data records exceeded 10% or more of the total records of any of the three components of wind velocity and/or CO_2 concentration. Quality of EC flux data was assured by selecting quality control flags 0 and 1 from EddyPro outputs [*Mauder and Foken*, 2006] and by rejecting the remaining anomalous flux data associated with dust, rain, or dew events. In addition, averaging periods with low turbulence were filtered out based

Table 1. Variables Measured in Balsa Blanca Together With the Sensors Used and Their Height

Variable	Sensor	Sensor Height
	Eddy Covariance System	
Wind speed (3-D) and sonic temperature	A three-axis sonic anemometer (CSAT-3, Campbell Scientific, Logan, UT, USA)	2.90 m
CO_2 and H_2O vapor densities	An open-path infrared gas analyzer (Li-Cor 7500, Lincoln, NE, USA)	2.90 m
	Meteorological and Soil Measurements	
Air pressure	An open-path infrared gas analyzer (Li-Cor 7500, Lincoln, NE, USA)	2.90 m
Photon flux density	Two photosynthetically active radiation sensors (Li-190, Li-Cor, Lincoln, NE, USA)	1.50 m
Net radiation	A net radiometer (NR Lite, Kipp&Zonen, Delft, Netherlands)	1.50 m
Air temperature	A thermohygrometer (HMP35-C, Campbell Scientific, Logan, UT, USA)	1.50 m
Air relative humidity	A thermohygrometer (HMP35-C, Campbell Scientific, Logan, UT, USA)	1.50 m
Soil water content	Four water content reflectometers (CS616, Campbell Scientific, Logan, UT, USA)	−5 cm
Soil temperature	Four soil temperature probes (TCAV, Campbell Scientific, Logan, UT, USA)	−5 cm
Rainfall	A tipping bucket (0.2 mm) rain gauge (785 M, Davis Instruments Corp., Hayward, CA, USA)	1.40 m

on a friction velocity (u_*) threshold estimated for each year by using the approach proposed by *Reichstein et al*. [2005]. The averaged u_* threshold for all the analyzed period (i.e., 2009–2013) was 0.15 m/s. The resulting fraction of daily and nocturnal missing NEE_{EC} data averaged for all years were 33 ± 13% and 74 ± 9%, respectively. However, assessment of the effect of rain pulses on NEE at ecosystem scale was performed with EC data for the drought period (defined below), and in addition, 70% of total rain pulses occurred during daytime, resulting in less missing NEE_{EC} data, approximately 25 ± 11%.

The net ecosystem carbon balances (NEE_{EC}) for both the year and the dry season were estimated by integrating the half-hourly CO_2 fluxes. Missing values were filled using the marginal distribution sampling technique [*Reichstein et al*., 2005]. Random uncertainty and errors in NEE_{EC} values introduced by the gap-filling process were calculated from the variance of the gap-filled data. The variance of the measured data was calculated by introducing artificial gaps and repeating the standard gap-filling procedure. Twice the standard deviation of sums of total data was taken as our NEE_{EC} error for the several time periods we used. Positive values of NEE_{EC} imply net CO_2 release to the atmosphere, while negative values represent net CO_2 uptake.

Regarding the rain pulse response analysis with EC data, dry seasons were defined as periods when a minimum volumetric soil water content (VWC_{soil}) of approximately 0.025 $m^3\ m^{-3}$ was observed, which

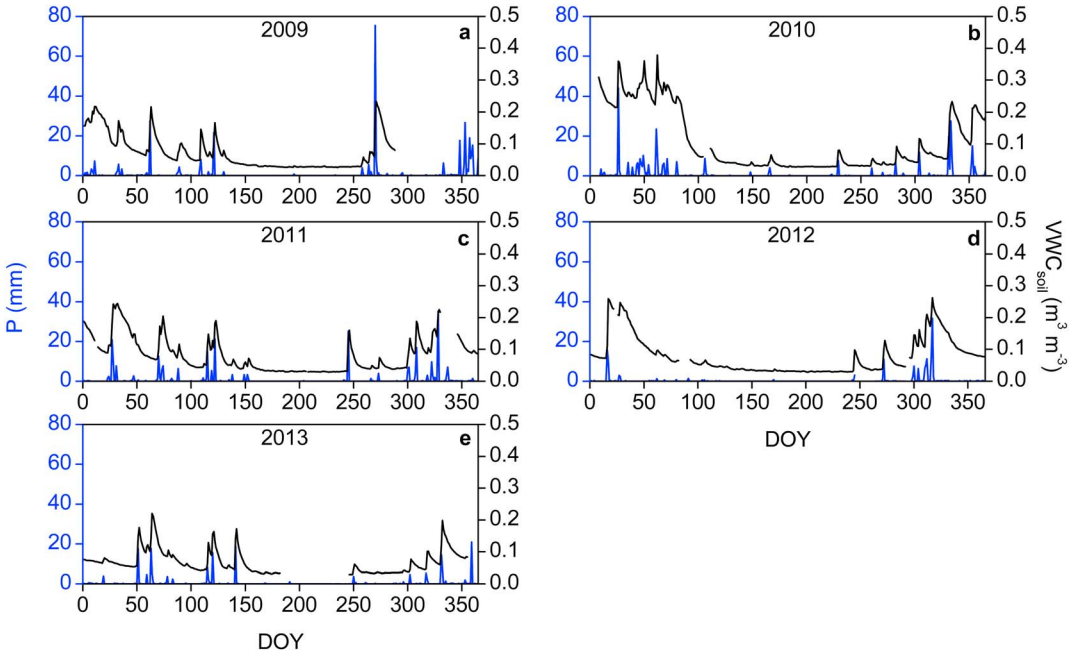

Figure 1. Time series of daily averaged soil water content (VWC_{soil}; $m^3\ m^{-3}$, black line) and precipitation (*P*; mm, blue line) in Balsa Blanca, for every year from 2009 to 2013.

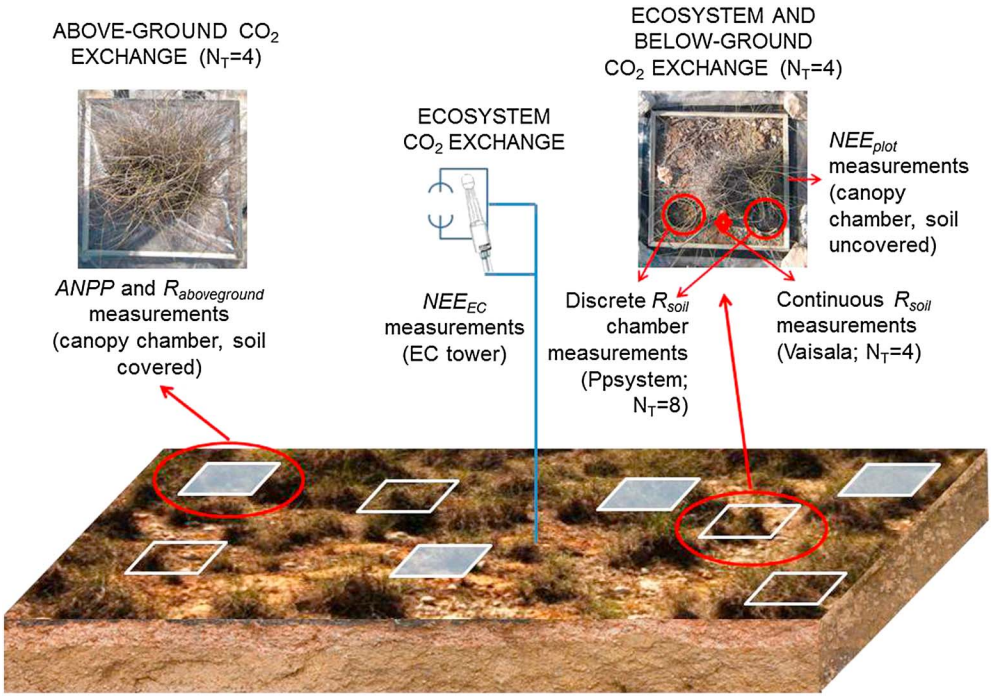

Figure 2. Diagram of the different methodologies used in this study in order to measure carbon exchanges at several spatial scales. Ecosystem CO_2 exchange is measured by the eddy covariance tower for several years, while the other CO_2 flux measurements were acquired during the rain pulse manipulation experiment.

usually began in the middle of July and ended in early November (Figure 1). Additionally, we considered that precipitation pulses were those precipitation events observable by VWC_{soil} sensors, which corresponded to >1 mm rainfall. We assessed the ecosystem response to rain pulse via the analysis of net ecosystem CO_2 fluxes during 7 days, from 1 day before the precipitation pulse to 5 days afterward. We excluded from our EC data analyses those half-hourly averaged EC values that corresponded to the moments when rainfall occurred in order to ensure the quality of the analyzed data. This period was selected after observing that the effect of most of rain pulses on NEE_{EC} disappears after 5 days.

2.3. Rain Pulse Manipulation Experiment

2.3.1. Experimental Design Overview

This section summarizes the experimental design; details for individual measurement systems appear in the subsections of the following section.

Eight plots of 0.25 m^2 containing a tussock grass of medium size and its surrounding soil area were randomly selected and demarcated in order to monitor aboveground, belowground, and net CO_2 exchanges during the rainfall manipulation experiment (Figure 2). On one hand, aboveground CO_2 exchanges, in light (aboveground net primary production, ANPP) and dark conditions (aboveground respiration, $R_{aboveground}$), were both measured in the same four plots with a portable canopy chamber excluding soil CO_2 effluxes by sealing around the bottom of the tussocks with a thick polyethylene sheet (Figure 2, top left). On the other hand, the remaining four plots were selected to measure soil as well as net CO_2 exchanges (R_{soil} and NEE_{plot}, respectively; Figure 2, top right), where NEE_{plot} fluxes were measured using the canopy chamber and discrete and continuous R_{soil} measurements were acquired by means of two different methodologies: soil respiration chambers were located on two PVC collars per plot (10 cm height, 10.5 cm diameter) to acquire discrete R_{soil} measurements, and volumetric soil CO_2 molar fraction, soil temperature, and volumetric soil water content were continuously measured by means of a CO_2 probe (GMM222, Vaisala, Helsinki, Finland), a temperature sensor (Decagon Devices, Inc., Pullman, WA, USA), and a ECH_2O sensor (EC-20, Decagon Devices, Inc., Pullman, WA, USA), respectively, in each of the four plots where the soil remained uncovered. These sensors were located at 5 cm depth, and data were collected every 5 min. All soil sensors were placed within the

experimental plots 1 month before the experiment in order to allow partial soil structure recovery. Soil properties alteration related to water channeling alongside the instrument was not observed during the experiment.

The experiment was conducted from 25 August (experiment day −1) to 29 August (experiment day 3) 2014, when meteorological conditions were similar and representative of the dry summer season in southeast Spain; concretely, no rainfall was registered since 24 June 2014. During day −1, the day prior to watering, we monitored aboveground, belowground, and net ecosystem CO_2 exchanges at the plot scale in order to characterize the ecosystem status under dry conditions. On day 0, the rain pulse was simulated in the early morning, when each plot was irrigated with 3.75 L of evenly distributed water with low mineralization, which corresponds to a precipitation event of 15 mm. Chamber measurement frequency was not constant during the whole experiment period. During the first two days (days −1 and 0), flux measurements were carried out approximately every hour in order to characterize diurnal variability before and immediately after the rain event. However, during days 1–3, measurements were carried out before solar noon since the photosynthetic activity of this species reached its maximum in early morning and became negligible around the central hours of the day [*Haase et al*., 1999; *Pugnaire et al*., 1996; *Ramírez*, 2006]. All the instrumentation was calibrated 1 month before the experiment.

2.3.2. Canopy and Soil Chamber Measurements

2.3.2.1. Canopy Chamber

A transparent transitory-state closure chamber ("canopy chamber") was used to measure ANPP, $R_{aboveground}$, and NEE_{plot}. Chamber dimensions were $50 \times 50 \times 60$ cm, and dark conditions, when measuring $R_{aboveground}$, were kept by covering with an opaque and reflective material to avoid light within the canopy chamber. The chamber system includes the following instrumentation: an infrared gas analyzer (Li-840, Li-Cor, Lincoln, NE, USA), two small fans (8.9 cm diameter), a thermocouple (PT100), and a data logger (CR1000, Campbell Sci., Logan, UT, USA). For each set of measurements, light condition measurements (i.e., ANPP and NEE_{plot} fluxes) were acquired approximately 1 h before dark condition measurements in order to minimize plant perturbations. We chose this approach because it is portable and allows rapid and accurate canopy flux measurements. More detailed information about canopy chamber design and methodology is given by *Pérez-Priego et al*. [2015].

2.3.2.2. Soil Chamber

A manual and portable opaque soil chamber system (EGM-4, PP-systems, Hitchin, UK) was used to acquire discrete measurements of soil CO_2 effluxes ($R_{soil\_ppsystem}$). For each measurement, the soil chamber was placed on a PVC collar during 120 s and CO_2 and water vapor molar fractions were recorded every 3 s.

2.3.2.3. Flux Calculation

For both chamber systems, the CO_2 fluxes were estimated from the initial slopes of CO_2 molar fractions of the confined air versus time, by using either linear or quadratic regression [*Kutzbach et al*., 2007; *Pérez-Priego et al*., 2010; *Wagner et al*., 1997] for the best regression fit. The raw values of CO_2 molar fraction were previously corrected for dilution [*Hubb*, 2012] from CO_2 molar fractions referred to wet air. Finally, the flux density was calculated using the ideal gas equation as explained by *Pérez-Priego et al*. [2015]. We rejected measurements acquired just after water addition to exclude data corresponding to the degasification process, namely, the displacement of CO_2-rich air from soil pores to the atmosphere due to water infiltration [*Inglima et al*., 2009; *Ma et al*., 2012; *Marañón-Jiménez et al*., 2011; *Wohlfahrt et al*., 2008; *Xu et al*., 2004].

2.3.3. Continuous Soil CO_2 Fluxes

The subsurface CO_2 molar fraction was continuously measured in each plot by CO_2 sensors (GMM222, Vaisala, Helsinki, Finland). Each probe was encased in a vertical PVC pipe open at the bottom, buried to a depth of 5 cm and sealed on the upper part by a rubber gasket. Sampling frequency was 1 Hz, and 5 min averages were stored in a data logger (CR3000, Campbell Sci., Logan, UT, USA). The CO_2 molar fraction readings were corrected for variations in soil temperature and atmospheric pressure. The soil CO_2 efflux ($R_{soil\_vaisala}$) was estimated according to the gradient method described by *Sánchez-Cañete and Kowalski* [2014].

2.3.4. Statistical Analysis

We applied different statistical tests to analyze the effect of the rain pulse over the different CO_2 fluxes measured at ecosystem and plot scales. On one hand, the one-way analysis of variance (ANOVA) test was applied to EC data in order to analyze the time response of the semiarid grassland C balance after rain pulses. On the other hand, we used the repeated-measurements ANOVA test to evaluate the effect of irrigation, in terms of

Table 2. Contribution of Carbon Emitted After Rain Pulse Events Over the Total Carbon Emitted During the Dry Season[a]

Year	Annual NEE_{EC} ($g\,C\,m^{-2}$)	Dry Season NEE_{EC} ($g\,C\,m^{-2}$)	Total Rain Pulses Dry Season	Total Rainfall Dry Season (mm)	NEE_{EC} After Rain Pulses ($g\,C\,m^{-2}$)	$\frac{C_{rain\ pulse}}{C_{dry\ season}}$ (%)
2009	43 ± 8	51 ± 4	7	89	30 ± 2	58
2010	−42 ± 8	37 ± 6	6	24	17 ± 2	46
2011	−67 ± 7	48 ± 4	4	36	17 ± 2	36
2012	67 ± 7	73 ± 4	5	20	30 ± 2	41
2013	−23 ± 7	22 ± 4	1	4	2 ± 1	9
Avg ± SD	−4 ± 57	46 ± 19	5 ± 2	35 ± 33	19 ± 12	38 ± 18
CV (%)	−1297	41	50	94	60	48

[a]Dry season corresponds to the period DOY = 200–310. Rain pulses correspond to rainfall >1 mm. Carbon emitted during the 5 days after rain pulse events was quantified and compared with the dry season carbon balance. Uncertainty of NEE_{EC} is related to gap-filling procedure. Average, standard deviation, and coefficient of variation (Avg, SD, and CV, respectively) are presented in the last three rows. Positive values indicate carbon release, while negative values mean carbon uptake.

time (i.e., days before and after rain pulse) as the fixed factor, over NEE_{plot}, ANPP, R_{soil}, and $R_{aboveground}$ since we directly measured every flux component in four plots over the 5 days of the experiment. For all the repeated-measurements ANOVA analysis, the Mauchly sphericity test indicated that the sphericity assumption was not fulfilled; therefore, we used the Huynh-Feldt approach to correct degrees of freedom. Additionally, in both cases, we investigated the differences between pairs of groups (i.e., CO_2 fluxes) via Bonferroni post hoc test. The statistical parameters obtained were F ratio ($F(DF_M, DF_R)$), together with the model and residual degrees of freedom (DF_M and DF_R, respectively), P value, and partial eta squared (η^2_p).

3. Results

3.1. Eddy Covariance Fluxes and Rain Pulse Events

Eddy covariance CO_2 fluxes in Balsa Blanca reveal that although annual NEE_{EC} varies widely from acting as a carbon (C) source or C sink over the period 2009–2013, net CO_2 emissions occur during the dry season for all years (Table 2). In fact, during the dry season, more than 80% of all days correspond to daytime C emissions. Additionally, precipitation pulses systematically provoke greater net emission of CO_2 over the short term (days to weeks; Figure 3). As shown in Table 2, an important amount of the total C emitted during the dry

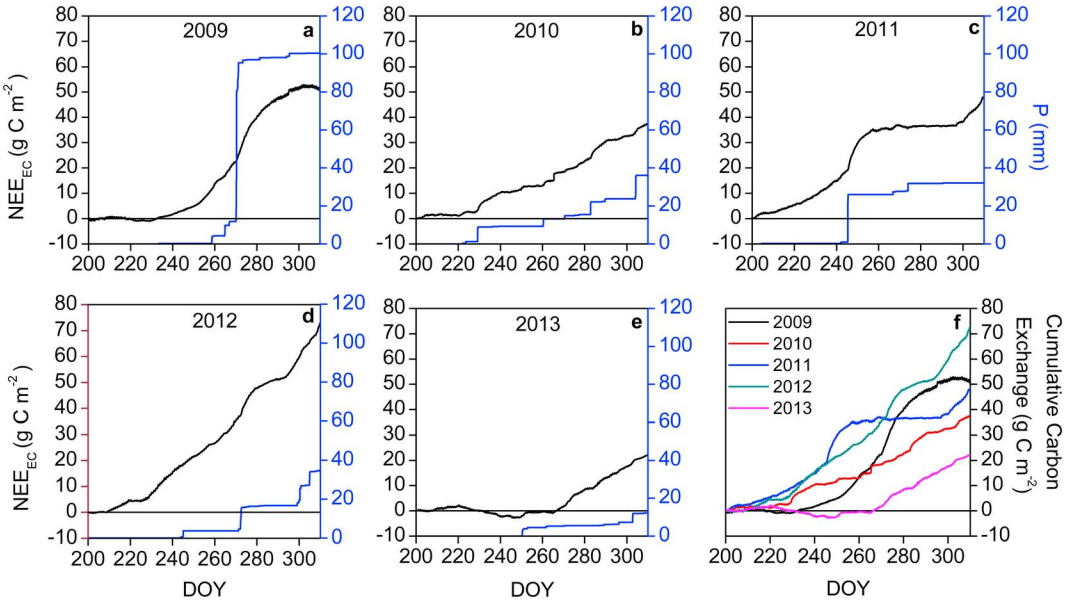

Figure 3. Cumulative dry season (day of year (DOY) = 200–310) net ecosystem carbon exchange measured with eddy covariance tower (NEE_{EC}; $g\,C\,m^{-2}$) and cumulative precipitation (P; mm) in Balsa Blanca, for every year from 2009 to 2013.

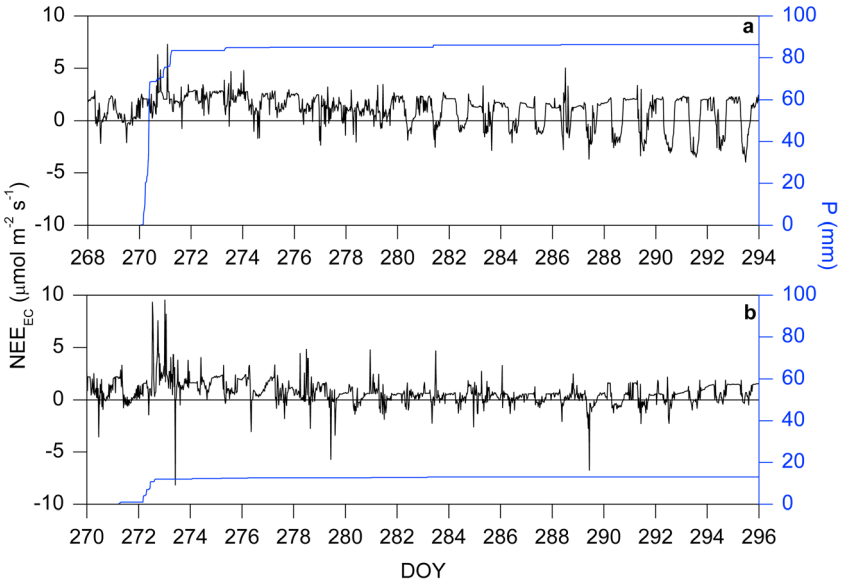

Figure 4. Half-hour averages of net ecosystem carbon exchange (NEE_{EC}; $\mu mol\ m^{-2}\ s^{-1}$, black line) and accumulated precipitation (*P*; mm, blue line). (a) An extreme rain pulse (27 September 2009) and (b) a small rain pulse (28 September 2012). Positive values indicate CO_2 release, and negative values mean CO_2 uptake.

season corresponds to CO_2 released in the first 5 days following precipitation. On average, although precipitation pulse responses represent only 7% of the dry season length, approximately 40% of the C emitted during the dry season corresponds to ecosystem CO_2 release registered after these precipitation events. In this regard, in 2009, the highest number of pulse events together with the highest amount of total rainfall resulted in a release of 58% of total C emitted during postpulse episodes comprising just 11% of the dry season period. Similarly, in 2010–2012, a relevant number of rain events caused 36–46% of the total C emission during 6–10% of the dry season period, while in 2013, far fewer and smaller rain pulses occurred, which corresponded to 9% of the total C emitted over just 2% of the dry season. Regarding interannual variability (Table 2), annual NEE_{EC} shows the highest coefficient of variation (CV = 1297) compared to NEE_{EC} during dry season (CV = 41) and after rain pulses (CV = 60) and also compared to the fraction of C loss following rain events over the total C amount emitted during dry season. Total amount of rainfall corresponding to rain pulses is also highly variable among years (CV = 94).

In Figure 3, we can notice that moderate and large precipitation pulses produced sudden and great increases in C emissions that returned to neutral progressively over several days after watering, as can be seen for some of the rain pulses occurring in 2010–2012 (Figures 3b–3d, respectively). Additionally, in 2009, when the highest rain pulse occurred (83 mm) over 2009–2013, we also detect net C uptake several weeks after precipitation (negative slope; Figure 3a). In contrast, small rain pulses triggered slight increases in C emission rates, as occurred in 2010 and 2013 (Figures 3b and 3e). Overall, rain pulses influence the pattern of net C emission over the dry season for 2009–2013 by increasing C release rates (Figure 3f).

It is evident that rain pulse magnitude is an important factor that determines the NEE_{EC} response (Figures 3 and 4). Based on our results, high-magnitude rain pulses (≥20 mm) can enable net CO_2 uptake since they generate a reserve of available water for several days enabling plants to upregulate and then carry out photosynthesis. For instance, the 83 mm rain pulse of 27 September 2009 (Figure 4a) caused CO_2 release during the subsequent 7 days, but then NEE_{EC} became neutral and afterward started—on the tenth day after abundant rainfall—to show diurnal net assimilation patterns with maximum uptake rates of approximately 4 $\mu mol\ m^{-2}\ s^{-1}$. In contrast, low-magnitude rain pulses (<10 mm), such as that of 28 September 2012 (Figure 4b), do not trigger net CO_2 uptake. However, this far lesser rainfall also readily provoked net emission of CO_2 of approximately 3 $\mu mol\ m^{-2}\ s^{-1}$ over a 7 day interval until NEE_{EC} returned to near-neutral levels.

Consequently, the overall effect of precipitation pulses on the C balance of our semiarid site depends on the amount of rainfall in each pulse. In this context, the rain pulse magnitude distribution (Figure 5) highlights the

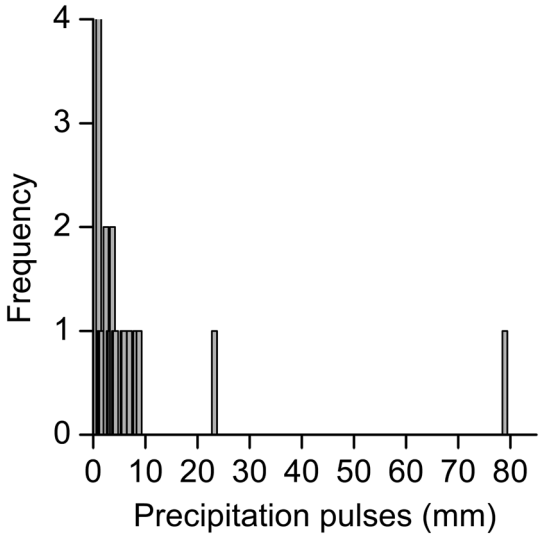

Figure 5. Absolute frequency distribution of magnitudes of rain pulses occurring during the dry season (DOY = 200–310) over a 5 years period (2009–2013).

higher occurrence of low-magnitude rain pulses (i.e., <10 mm) that commonly trigger net CO_2 emission, as shown before. In fact, when we examine the short-term effect of rain pulses over the measured NEE_{EC} for the whole study period (i.e., dry seasons of 2009–2013) at the diurnal time scale (Figure 6), we see that net C emission predominates, reaching its maximum during the first 24 h after the rain pulse. During subsequent days, NEE_{EC} decreases in magnitude and reaches values quite similar to those occurring the day before water input. The high variability of NEE_{EC} is related to the great amount of data used to calculate each averaged value, which corresponds to variable-magnitude rain pulses happening at different moments over the dry season (Figure 6). However, the ANOVA test results show that NEE_{EC} is significantly affected by rain pulses at the short term ($F(6, 91) = 2.724$; P value = 0.017), for the overall rain pulses that occurred over the whole study period (2009–2013). In addition, based on Bonferroni test results, there is a significant difference between the day after the rain pulse (day 1), when the highest ecosystem CO_2 flux rate occurs, compared to the rest of the days.

3.2. Rain Pulse Manipulation Experiment

On one hand, we analyze the pulse response evolution for every NEE component based on the plot-scale flux measurements acquired during the manipulation experiment. Generally, during the whole 5 day experiment, R_{soil} measured with soil respiration chambers (i.e., $R_{soil\_ppsystem}$) and R_{soil} measured with soil CO_2 concentration sensors ($R_{soil\_vaisala}$) agreed by showing similar CO_2 flux values and patterns (Figure 7), so hereinafter we will occasionally refer to both variables as if they were the same (i.e., R_{soil}). During the prepulse day (day −1), average NEE was low but positive (0.25 μmol m^{-2} s^{-1}), with R_{soil} being the predominant component

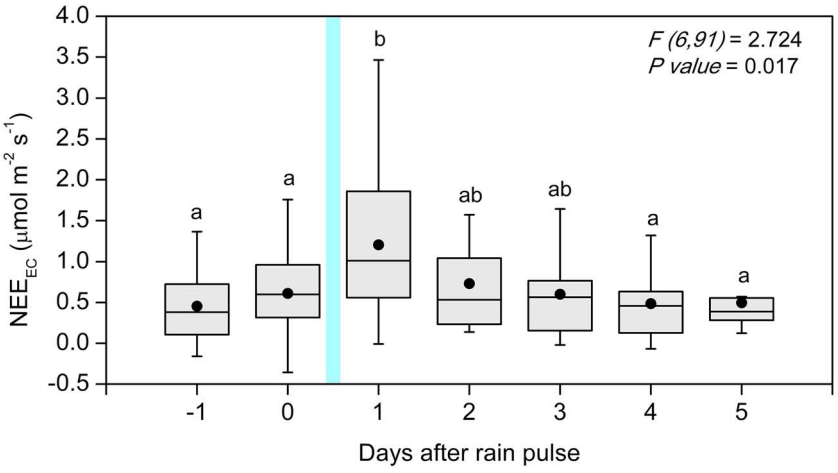

Figure 6. Box-and-whisker plots of diurnal ecosystem responses after an averaged rain pulse of 5 ± 5 mm (blue bar) in terms of net ecosystem carbon exchange measured with eddy covariance (NEE_{EC}; μmol CO_2 m^{-2} s^{-1}). Every flux data point corresponds to the diurnal average of half-hour NEE_{EC} fluxes after every rain pulse that occurred during the drought periods (DOY = 200–310) of years 2009–2013. Positive values indicate CO_2 release. Results of one-way ANOVA test (F ratio and P value) and post hoc Bonferroni test (letters above the box charts) are shown in the graph; the significance level is 95% ($\alpha = 0.05$).

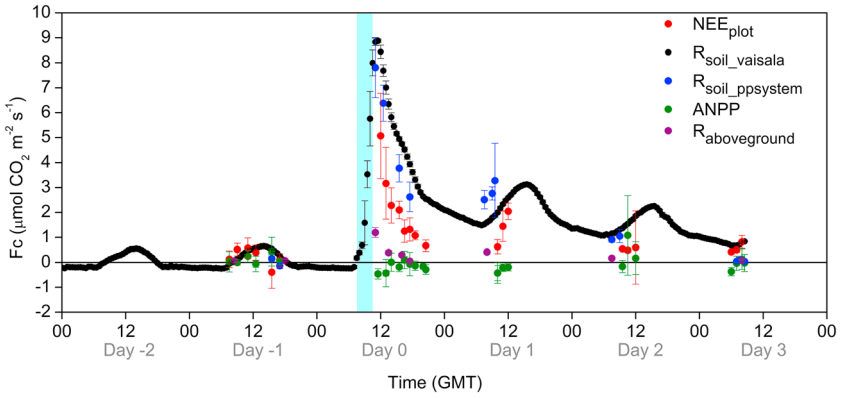

Figure 7. Averaged ($n = 4$) CO_2 fluxes (Fc; µmol m^{-2} s^{-1}) of net ecosystem carbon exchange at plot scale (NEE_{plot}; red data points), aboveground net primary production (ANPP; green data points), aboveground respiration ($R_{aboveground}$), and belowground or soil respiration fluxes, obtained with soil chambers ($R_{soil\_ppsystem}$; blue data points) and with soil CO_2 concentration sensors ($R_{soil\_vaisala}$; black data points), all measured during the 5 days of the experiment (25–29 August 2014), one before and four after the simulated rain pulse of 15 mm (blue bar on day 0). Positive values indicate CO_2 release, while negatives values mean CO_2 uptake. Error bars are ± SD.

comprising 61% of the NEE magnitude (Figure 8c). On day 0, we irrigated each plot with 15 mm, and afterward, NEE was 1 order of magnitude higher than on the previous day (approximately 10 µmol m^{-2} s^{-1}) and, likewise, R_{soil} was the prevailing component constituting 82% of the overall net C release, while $R_{aboveground}$ only comprised 13% (Figure 8d). On day 1 (i.e., first day after the pulse), NEE decreased 64%, with R_{soil} and $R_{aboveground}$ prevalent as on day 0. Contrary to previous days, on day 2, despite the great variability

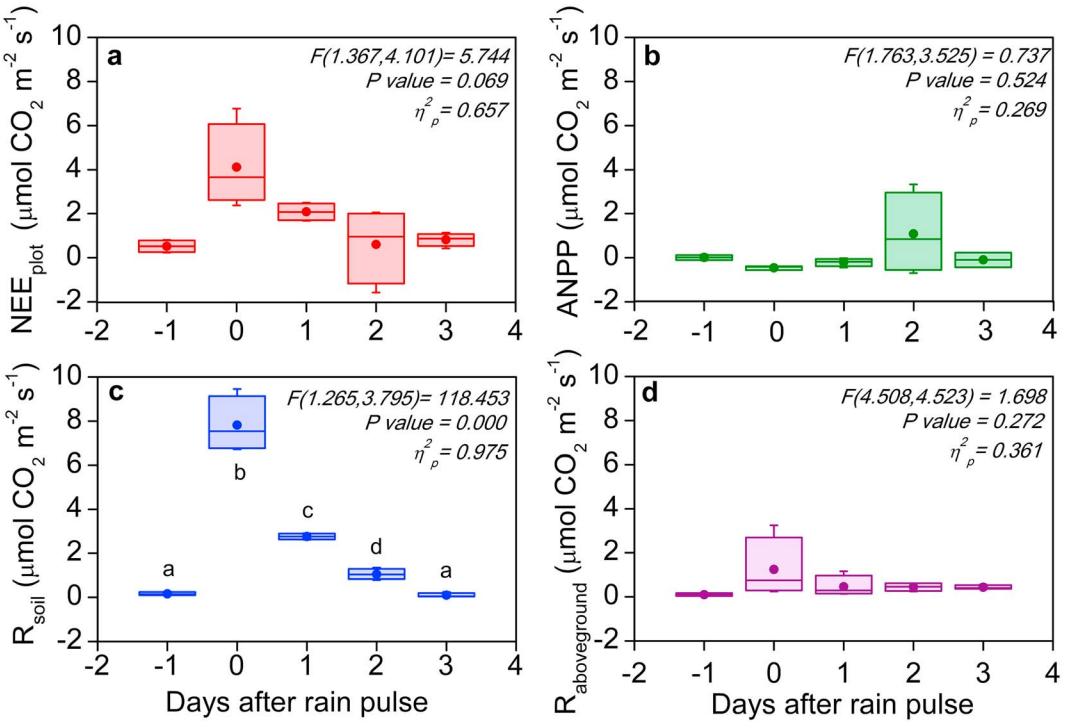

Figure 8. Box-and-whisker plots of CO_2 fluxes (µmol m^{-2} s^{-1}) of (a) net ecosystem carbon exchange at plot scale (NEE_{plot}; red box charts), (b) aboveground net primary production (ANPP; green box charts), (c) belowground or soil respiration (R_{soil}; blue box charts) measured with chambers, and (d) aboveground respiration ($R_{aboveground}$) for the 5 days long rain pulse manipulation experiment. Results of the one-way ANOVA test for repeated measurements (F ratio and P value) and the post hoc Bonferroni test (letters above the box charts) are shown in every graph ($n = 4$). For all the statistical analysis, the significance level is 95% ($\alpha = 0.05$) and Huynh-Feldt approach has been used to correct degrees of freedom.

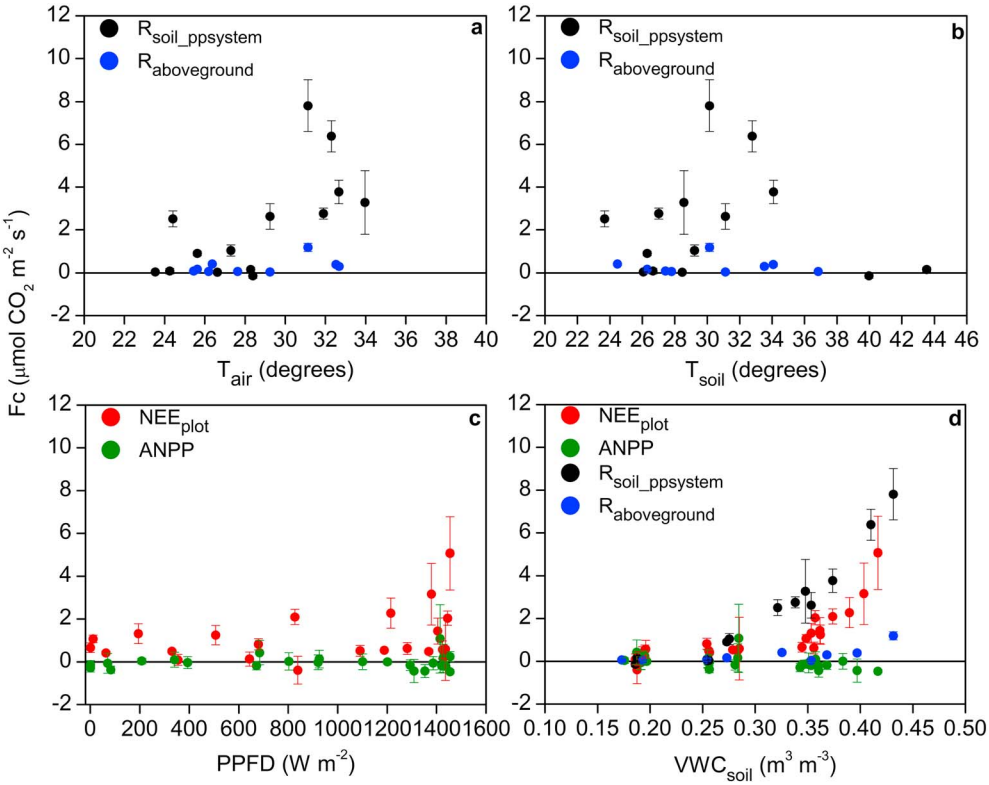

Figure 9. Relationship between meteorological variables and CO_2 fluxes measured during the 5 days long experiment performed in Balsa Blanca from 23 to 29 August 2015. Half-hour averages of (a) air temperature (T_{air}) versus aboveground respiration ($R_{aboveground}$) and soil respiration measured with chamber systems ($R_{soil\_ppsystem}$), (b) soil temperature (T_{soil}) versus aboveground respiration ($R_{aboveground}$) and belowground or soil respiration measured with chamber systems ($R_{soil\_ppsystem}$), (c) photosynthetically photon flux density (PPFD) versus inverse of aboveground net primary production (ANPP) and net ecosystem exchange (NEE_{plot}), and (d) volumetric soil water content (VWC_{soil}) versus all punctual measured CO_2 fluxes (NEE_{plot}, ANPP, $R_{soil\_ppsystem}$, and $R_{aboveground}$). All flux data are averages of four measurements. Positive values indicate CO_2 release, while negative values are CO_2 uptake. Error bars are ± SD.

measured among plots, the contribution of the average ANPP became as important as R_{soil}, each comprising 40% of NEE (Figure 8b). Additionally, $R_{aboveground}$ increased its prevalence up to 17%. Finally, on day 3 of the experiment, NEE became neutral (approximately 0.64 μmol m^{-2} s^{-1}), similar to the prepulse day.

Additionally, we elucidate whether the NEE components were significantly affected by rain pulses at the daily time scale (Figure 8). In this sense, results of the repeated-measurements ANOVA test applied to plot-scale NEE, ANPP, R_{soil}, and $R_{aboveground}$ showed that only R_{soil} was significantly affected by irrigation (F(1.27, 3.80) = 118.45; P value = 0.000; η^2_p = 0.98; Figure 8c). In fact, the Bonferroni test results demonstrated that daily R_{soil} fluxes were statistically different among days 0–2 (Figure 8c), while day −1 and day 3 were not different. On the other hand, NEE was also statistically affected at a lower significance level of 90% (F(1.37, 4.10) = 5.74; P value = 0.069; η^2_p = 0.49; Figure 8a). Additionally, we found significant differences between day −1 and the day after irrigation (day 1) as well as between days 1 and 3 but also at a lower significance level of 90%. In contrast, ANPP (F(1.76, 3.53) = 0.74; P value = 0.52; η^2_p = 0.27) and $R_{aboveground}$ (F(1.51, 4.52) = 1.70; P value = 0.27; η^2_p = 0.36) were not significantly affected by the rain event (Figures 8b and 8d).

The relationship between the common driving factors that determine CO_2 flux magnitudes over the experiment is modulated by soil water availability. Air temperature and soil temperature influence R_{soil} (i.e., $R_{soil\_ppsystem}$) only when soil is moist (Figures 9a and 9b). In fact, we can observe two distinct groups of points, one where R_{soil} fluxes are close to zero even for high soil temperatures of around 35–45°C (Figure 9b) and another where a hysteretic pattern may correspond to the days after irrigation (Figures 9a and 9b). Similarly, light sensitivity of ANPP fluxes uniquely exists in a few particular moments

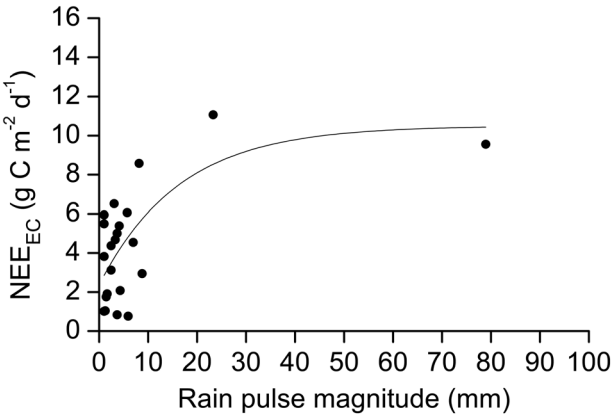

Figure 10. Rain pulse magnitudes versus cumulative net carbon ecosystem exchange measured with eddy covariance tower (NEE_{EC}) measured over the 5 days after every rain pulse registered during the dry season from 2009 to 2013. Coefficient of determination (R^2) equates to 0.38.

after irrigation, as very low values of ANPP are registered for a wide range of incident photosynthetically photon flux densities (PPFD; Figure 9c). Accordingly, NEE_{plot} measurements are more affected by increments in soil volumetric water content (VWC_{soil}), as well as R_{soil}, given the scant plant photosynthetic response to water addition.

4. Discussion

4.1. Precipitation Pulse Response of Ecosystem C Exchange

At the annual time scale, we have determined that drought conditions systematically entail CO_2 emission (Figure 3f), and concretely, Balsa Blanca emits approximately 50 g C m^{-2} during the dry season (Table 2). This has been also observed in other semiarid and arid ecosystems [*Aires et al*., 2008; *Baldocchi*, 2008; *Cleverly et al*., 2013; *Huxman et al*., 2004b; *Wohlfahrt et al*., 2008; *Yan et al*., 2011], especially in grass-dominated arid and semiarid ecosystems like Balsa Blanca [*Scott et al*., 2012]. This C loss stems from (1) significant gross primary product (GPP) reduction [*Scott et al*., 2012], (2) the presence of minimal but significant ecosystem respiration [*Cable et al*., 2012; *Ma et al*., 2012], and (3) the sudden increase in soil respiration (R_{soil}) when low- and medium-sized rain pulses occur [*Barron-Gafford et al*., 2011], as shown in this study (Figure 3). In this sense, we have quantified that annually, 40% of the CO_2 emitted during the dry season corresponds to CO_2 released during the 5 days subsequent to rain pulses, a period encompassing only 7% of the dry season length.

The effect of a precipitation pulse on a semiarid ecosystem C balance depends on the specific rain pulse attributes, such as magnitude (mm), which has been proposed to be one of the most determining factors affecting the ecosystem response [*Huxman et al*., 2004b]. Similar to previous studies in Mediterranean grasslands [*Aires et al*., 2008], we have found different responses after a small and a large rain pulse in our semiarid grassland. The selected large rain pulse (Figure 4a), which in total exceeded 80 mm, triggered net CO_2 assimilation, while the smaller one (approximately 13 mm; Figure 4b) did not correspond to a sufficient water supply to stimulate plant photosynthesis. Nonetheless, some studies suggest that a rain pulse of this magnitude could elicit net CO_2 uptake [*Huxman et al*., 2004b], while others state that small or even medium-sized rain events (e.g., 10–15 mm) only can provoke CO_2 release [*Aires et al*., 2008; *Lauenroth and Bradford*, 2012].

As observed in other water-limited ecosystems [*Baldocchi*, 2008; *Cleverly et al*., 2013; *Huxman et al*., 2004a; *Mayor et al*., 2011; *Schwinning and Sala*, 2004], most of the rain pulses registered in Balsa Blanca correspond to small or medium-sized precipitation events ($<$10 mm; Figure 5). Hence, precipitation events that occurred over the 2009–2013 dry seasons statistically enhanced net CO_2 emissions at the short term during the dry season, concretely, during 5 days after the rain pulse (Figure 6). Nevertheless, similar to other results [*Parton et al*., 2012], the relationship between the rain pulse magnitude and triggered net CO_2 emission during the dry season is complex, and thus, it is difficult to find a robust correlation (Figure 10). Additionally, it is important to notice the possible underestimation in NEE caused by the exclusion of half-hourly EC fluxes that corresponded to the moments when rainfall occurred, but given the brevity of the rainfall episodes, generally 0.5–1 h, the error caused by gap-filled data is minimal.

Accordingly, the decomposition of NEE becomes crucial to understand the complex ecosystem response composed of several biotic processes and, consequently, to provide quantitative evidence of whether photosynthesis as well as soil respiration activate after irrigation.

4.2. Short-Term Pulse Response of NEE Components

On one hand, our experimental results revealed that despite differences in the contribution of the NEE components among days of experiment, only R_{soil} was significantly affected by the addition of 15 mm.

During the prepulse and third day of experiment, we observed similar and low R_{soil} rates (i.e., 0–1 $\mu mol\, m^{-2}\, s^{-1}$). Such slight soil respiration rates have been related to the lack of soil moisture that inhibits heterotrophic respiration [*Baldocchi*, 2008; *Cable et al*., 2012; *Yan et al*., 2011], and to the limitation of substrates due to GPP reduction [*Cleverly et al*., 2013], given the link between productivity and ecosystem respiration [*Janssens et al*., 2001; *Migliavacca et al*., 2011]. Nevertheless, despite the absence of water in the soil, minimum daily respiration rates have been observed whose diurnal pattern shows a maximum at noon [*Ma et al*., 2012; *Scott et al*., 2010], similar to our results.

During the pulse day (day 0) we measured the highest R_{soil} and irrigation explained the 98% of the Rsoil variance ($\eta^2_p = 0.98$). Under drought conditions, many studies have also reported an immediate increase in R_{soil} following rain pulses [*Carbone et al*., 2011; *Huxman et al*., 2004a; *Jarvis et al*., 2007; *Leon et al*., 2014; *Sponseller*, 2007; *Thomey et al*., 2011; *Wohlfahrt et al*., 2008], as observed in this study (Figure 6). This effect on R_{soil} has been attributed to the Birch effect, which corresponds to the activation of soil respiration with the consequent mineralization of organic matter and CO_2 release [*Birch*, 1959].

Then, 2 days after water addition, R_{soil} effluxes decrease significantly compared to day 0. The progressive decline of R_{soil}, after the first peak following a rain pulse, may be related to the depletion of water in soil pores as well as the reduction in soil labile organic matter. In this regard, prior to the rainfall event, the process of photodegradation can provide the amount of organic carbon needed to allow this peak in soil respiration, since it is known that there is accumulation of dead biomass around *Machrocloa* sp. tussocks [*Maestre et al*., 2009] that is susceptible to partial degradation under conditions of high UV radiation, dry soil, and high temperature during drought periods [*Ma et al*., 2012; *Rutledge et al*., 2010].

On the other hand, contrary to our hypothesis, aboveground processes (i.e., ANPP and $R_{aboveground}$) were not significantly affected by the rain pulse. Despite the higher contribution of $R_{aboveground}$ (13%) and ANPP (40%) over NEE, on day 0 and day 2, respectively, neither variable was significantly pulse affected due the great variability among plot values. However, for larger rain pulses, *Pugnaire et al*. [1996] detected the activation of the photosynthetic apparatus of *Machrocloa* sp. after a simulated rain pulse of 31 mm, double the amount of water added in our study. Consequently, we suggest that after prolonged drought, only large rainfall amounts ($\geq$20 mm) are able to break the dormancy period where *Machrocloa* sp. plants remain photosynthetically inactive. This might be related to any of many morphological and physiological strategies of this species against drought that lead to the insufficient presence of active leaves to carry out photosynthesis. These include low elasticity of cell walls [*Pugnaire and Haase*, 1996], regulation of stomatal conductance [*Haase et al*., 1999], photoinhibition [*Balaguer et al*., 2002; *Pugnaire et al*., 1996], photoprotection [*Pugnaire and Haase*, 1996], photorespiration [*Balaguer et al*., 2002; *Bohnert and Jensen*, 1996; *Foyer and Noctor*, 2000; *Wingler et al*., 2000], leaf folding [*Rychnovská*, 1964], leaf pigment loss [*Ramírez*, 2006], and leaf angle modification [*Valladares and Pugnaire*, 1999]. Additionally, *Huxman et al*. [2004b] highlighted the relevance of infiltration depth as a factor determining plant activation after rain pulses, but in our case, this cannot play a key role because *Machrocloa* sp. is a shallow-rooted species [*Maestre et al*., 2007].

Finally, regarding our study results, negative values of nocturnal R_{soil} fluxes estimated from the Vaisala probes ($R_{soil\_vaisala}$; Figure 7) were detected during previous days before irrigation and turned into positive after irrigation (Figure 6). Similar results were found by means of both a multichamber soil respiration monitoring system and soil CO_2 Vaisala probes located in the soil subsurface within a Chihuahuan desert shrubland that also features a caliche horizon [*Hamerlynck et al*., 2013]. They observed negative nocturnal soil CO_2 effluxes under drought conditions that became positive during the monsoon season. These authors related these negative soil fluxes to processes of carbonate dissolution, which might also happen in Balsa Blanca where there is a petrocalcic horizon too. On the other hand, at some specific moments throughout the experiment, we found that the difference between R_{soil} and ANPP exceeds measured NEE by approximately 1 $\mu mol\, m^{-2}\, s^{-1}$. This fact might be due to the accuracy of the different sensors and methodologies used to acquire these flux measurements. Apart from that, we can conclude from our experiment results that the highest increase in CO_2 emission occurs in a short time period, (from minutes to a few hours; Figure 7) following the rain pulse, and sometimes (for small rain pulses) this emission peak may be smoothed in a half-hourly averaged EC value.

4.3. General Discussion

In our study, we highlight the strength of EC data to measure the long-term effect of rain pulses on NEE as well as to assess its high interannual variability (Table 2). However, by using solely the EC technique, we

cannot track biological processes composing the overall NEE, and hence, we present the experimental results to complement EC results at the short term. However, the experiment was limited in order to determine the threshold magnitude needed to trigger photosynthesis (due to the short duration and the unique rain pulse magnitude simulated). Nevertheless, we have demonstrated that CO_2 emission is significant (Table 2) during the dry season and highly modulated by the rain pulses that enhance this C loss (Figures 3 and 6) through the activation of soil respiration (Figures 7 and 8c).

Overall, future climate projections point to decreases in water availability via decreases in rain events and total precipitation in some regions [*Beier et al*., 2012; *Intergovernmental Panel on Climate Change* (*IPCC*), 2007] including the Mediterranean basin [*Solomon et al*., 2009]. Concurrently, this indicates an alteration of rainfall distribution that likely implies variation in the size, frequency, and intensity of future rain pulses [*Cleverly et al*., 2013; *IPCC*, 2012] in such arid and semiarid regions. In this regard, the occurrence of stochastic precipitation pulses within long dry periods might mostly provoke the activation of soil respiration processes in arid and semiarid ecosystems. Hence, a precipitation distribution characterized by low-frequency and low-magnitude events would lead to CO_2 release, while anomalous high-magnitude and low-frequency events might cause intermittent CO_2 uptake over several days, as shown in this study. In contrast, high-frequency events may support continuous photosynthetic activity as well as soil respiration, with the overall biological activity being proportional to the amount of stored water in the soil (up to saturation). In this way, the capability of semiarid ecosystems to act as C sinks would be enhanced. Nevertheless, more research is still needed to accurately characterize the dimension and sense of C balance variability in drylands regarding their response to climate change. This is especially so when the aim of building applicable modeling approaches in drylands is considered as imperative in order to predict, mitigate, and adapt to future climatic and environmental scenarios.

5. Conclusions

Rain pulses, occurring during the dry season, are a frequent form of water input in semiarid ecosystems and an important climatic factor affecting the C balance of water-limited ecosystems. In the studied semiarid grassland, the net CO_2 emitted to the atmosphere triggered by rain pulse events contributed from 9 to 58% to the total net CO_2 release measured with eddy covariance, despite comprising just 2 to 11% of the dry season period length for five study years (2009–2013). The main biological process determining the NEE response after a rain pulse is soil respiration, given the higher occurrence of small- and medium-sized rain events that may be not sufficient to enable plant photosynthesis. However, net CO_2 uptake patterns can be observed when infrequent and large rainfall events occur. The manipulation pulse experiment results showed that only R_{soil} was significantly affected by the rain pulse. However, the contribution of the different components to the overall NEE changed over the experiment days. In this regard, R_{soil} was distinctly dominant during the pulse day and the day afterward (approximately 80% of the NEE), whereas ANPP seemed to become more prevalent during the second day following irrigation (approximately 40% of NEE), despite the great variability in the measurements.

Global estimations of temperature and precipitation regimes point to an increase of drought periods and extreme precipitation events that might imply an increase in the net CO_2 emission in semiarid regions. Therefore, the characterization of the responses of biological components of the C balance to rain pulses becomes crucial in order to improve current climatic modeling schemes and also to design proper mitigation policies.

Acknowledgments

A. López-Ballesteros acknowledges support from the Spanish Ministry of Economy and Competitiveness (FPI grant, BES-2012-054835). This research was funded in part by the Spanish Ministry of Economy and Competitiveness projects CARBORAD (CGS2011-27493), ICOS-SPAIN (AIC10-A-000474), SOILPROF (CGL2011-15276-E), GEISpain (CGL2014-52838-C2-1-R), and also by the international project DIESEL (PEOPLE-2013-IOF-625988). Eddy covariance data used in this work are available in FLUXNET database, and experimental data are available by contacting with the corresponding author. We thank M.G. Valdecasas-Ojeda for her programming advice and also C. Lopez for his help in the field work. Comments from Russell L. Scott improved this paper significantly. Thanks also go to the anonymous reviewers whose remarks improved this manuscript.

References

Ahlström, A., et al. (2015), The dominant role of semi-arid ecosystems in the trend and variability of the land CO_2 sink, *Science*, *348*(6237), 895–899.

Aires, L. M. I., C. A. Pio, and J. S. Pereira (2008), Carbon dioxide exchange above a Mediterranean C3/C4 grassland during two climatologically contrasting years, *Global Change Biol.*, *14*(3), 539–555.

Balaguer, L., F. I. Pugnaire, E. Martínez-Ferri, C. Armas, F. Valladares, and E. Manrique (2002), Ecophysiological significance of chlorophyll loss and reduced photochemical efficiency under extreme aridity in *Stipa tenacissima L*, *Plant Soil*, *240*(2), 343–352.

Baldocchi, D. (2008), TURNER REVIEW No. 15. "Breathing" of the terrestrial biosphere: Lessons learned from a global network of carbon dioxide flux measurement systems, *Aust. J. Bot.*, *56*(1), 1–26.

Barron-Gafford, G. A., R. L. Scott, G. D. Jenerette, and T. E. Huxman (2011), The relative controls of temperature, soil moisture, and plant functional group on soil CO_2 efflux at diel, seasonal, and annual scales, *J. Geophys. Res.*, *116*, G01023, doi:10.1029/2010JG001442.

Beier, C., et al. (2012), Precipitation manipulation experiments—Challenges and recommendations for the future, *Ecol. Lett.*, *15*(8), 899–911.

Birch, H. F. (1959), The effect of soil drying on humus decomposition and nitrogen availability, *Plant Soil*, *10*(1), 9–31.

Bohnert, H. J., and R. G. Jensen (1996), Strategies for engineering water-stress tolerance in plants, *Trends Biotechnol.*, *14*(3), 89–97.
Cable, J. M., G. A. Barron-Gafford, K. Ogle, M. Pavao-Zuckerman, R. L. Scott, D. G. Williams, and T. E. Huxman (2012), Shrub encroachment alters sensitivity of soil respiration to temperature and moisture, *J. Geophys. Res.*, *117*, G01001, doi:10.1029/2011JG001757.
Carbone, M. S., C. J. Still, A. R. Ambrose, T. E. Dawson, A. P. Williams, C. M. Boot, S. M. Schaeffer, and J. P. Schimel (2011), Seasonal and episodic moisture controls on plant and microbial contributions to soil respiration, *Oecologia*, *167*(1), 265–278.
Charley, J. L., and N. E. West (1975), Plant-induced soil chemical patterns in some shrub-dominated semi-desert ecosystems of Utah, *J. Ecol.*, *63*, 945–963.
Cleverly, J., N. Boulain, R. Villalobos-Vega, N. Grant, R. Faux, C. Wood, P. G. Cook, Q. Yu, A. Leigh, and D. Eamus (2013), Dynamics of component carbon fluxes in a semi-arid Acacia woodland, central Australia, *J. Geophys. Res. Biogeosci.*, *118*, 1168–1185, doi:10.1002/jgrg.20101.
Cross, A., and W. Schlesinger (1999), Plant regulation of soil nutrient distribution in the northern Chihuahuan Desert, *Plant Ecol.*, *145*(1), 11–25.
Ehleringer, J. R., S. Schwinning, and R. Gebauer (1999), Water-use in arid land ecosystems, in *Plant Physiological Ecology*, edited by M. C. Press et al., pp. 347–365 , Blackwell, Edinburgh.
Fan, J., S. Jones, L. Qi, Q. Wang, and M. Huang (2012), Effects of precipitation pulses on water and carbon dioxide fluxes in two semiarid ecosystems: Measurement and modeling, *Environ. Earth Sci.*, *67*(8), 2315–2324.
Foyer, C. H., and G. Noctor (2000), Tansley Review No. 112. Oxygen processing in photosynthesis: Regulation and signalling, *New Phytol.*, *146*(3), 359–388.
Haase, P., F. I. Pugnaire, S. C. Clark, and L. D. Incoll (1999), Environmental control of canopy dynamics and photosynthetic rate in the evergreen tussock grass *Stipa tenacissima*, *Plant Ecol.*, *145*(2), 327–339.
Hamerlynck, E. P., R. L. Scott, E. P. Sánchez-Cañete, and G. A. Barron-Gafford (2013), Nocturnal soil CO_2 uptake and its relationship to subsurface soil and ecosystem carbon fluxes in a Chihuahuan Desert shrubland, *J. Geophys. Res. Biogeosci.*, *118*, 1593–1603, doi:10.1002/2013JG002495.
Hubb, J. (2012), The importance of water vapour measurements and corrections LI-COR Biosciences Inc. Application Note, 129, pp. 8.
Huxman, T. E., J. M. Cable, D. D. Ignace, J. A. Eilts, N. B. English, J. Weltzin, and D. G. Williams (2004a), Response of net ecosystem gas exchange to a simulated precipitation pulse in a semi-arid grassland: The role of native versus non-native grasses and soil texture, *Oecologia*, *141*(2), 295–305.
Huxman, T. E., K. A. Snyder, D. Tissue, A. J. Leffler, K. Ogle, W. T. Pockman, D. R. Sandquist, D. L. Potts, and S. Schwinning (2004b), Precipitation pulses and carbon fluxes in semiarid and arid ecosystems, *Oecologia*, *141*(2), 254–268.
Inglima, I., G. Alberti, T. Bertolini, F. P. Vaccari, B. Gioli, F. Miglietta, M. F. Cotrufo, and A. Peressotti (2009), Precipitation pulses enhance respiration of Mediterranean ecosystems: The balance between organic and inorganic components of increased soil CO_2 efflux, *Global Change Biol.*, *15*(5), 1289–1301.
Intergovernmental Panel on Climate Change (IPCC) (2007), *Climate Change 2007: Synthesis Report. Contribution of Working Groups I, II and III to the Fourth Assessment Report of the Intergovernmental Panel on Climate Change*, edited by Core Writing Team, R. K. Pachauri, and A. Reisinger, pp. 104, IPCC, Geneva, Switz.
Intergovernmental Panel on Climate Change (IPCC) (2012), Summary for policymakers, in *Managing the Risks of Extreme Events and Disasters to Advance Climate Change Adaptation. A Special Report of Working Groups I and II of the Intergovernmental Panel on Climate Change*, edited by C. B. Field et al., pp. 1–19, Cambridge Univ. Press, Cambridge, U. K., and New York.
Janssens, I. A., et al. (2001), Productivity overshadows temperature in determining soil and ecosystem respiration across European forests, *Global Change Biol.*, *7*, 269–278.
Jarvis, P., et al. (2007), Drying and wetting of Mediterranean soils stimulates decomposition and carbon dioxide emission: The "Birch effect", *Tree Physiol.*, *27*(7), 929–940.
Jenerette, G. D., R. L. Scott, and T. E. Huxman (2008), Whole ecosystem metabolic pulses following precipitation events, *Funct. Ecol.*, *22*(5), 924–930.
Kutzbach, L., J. Schneider, T. Sachs, M. Giebels, H. Nykänen, N. J. Shurpali, P. J. Martikainen, J. Alm, and M. Wilmking (2007), CO_2 flux determination by closed-chamber methods can be seriously biased by inappropriate application of linear regression, *Biogeosciences*, *4*(6), 1005–1025.
Lauenroth, W. K., and J. B. Bradford (2012), Ecohydrology of dry regions of the United States: Water balance consequences of small precipitation events, *Ecohydrology*, *5*(1), 46–53.
Lázaro, R., F. S. Rodrigo, L. Gutiérrez, F. Domingo, and J. Puigdefábregas (2001), Analysis of a 30-year rainfall record (1967–1997) in semi–arid SE Spain for implications on vegetation, *J. Arid Environ.*, *48*(3), 373–395.
Le Houérou, H. N. (1986), The desert and arid zones of Northern Africa, in *Ecosystems of the World 12B. Hot Deserts and Arid Shrublands B*, edited by M. Evenary, I. Noy-Meir, and D. W. Goodall, Elsevier, Amsterdam.
Leon, E., R. Vargas, S. Bullock, E. Lopez, A. R. Panosso, and N. La Scala (2014), Hot spots, hot moments, and spatio-temporal controls on soil CO_2 efflux in a water-limited ecosystem, *Soil Biol. Biochem.*, *77*, 12–21.
Li, F., W. Zhao, and H. Liu (2013), The response of aboveground net primary productivity of desert vegetation to rainfall pulse in the temperate desert region of Northwest China, *PLoS One*, *8*(9), e73003.
Ma, S., D. D. Baldocchi, J. A. Hatala, M. Detto, and J. Curiel Yuste (2012), Are rain-induced ecosystem respiration pulses enhanced by legacies of antecedent photodegradation in semi-arid environments?, *Agric. For. Meteorol.*, *154–155*, 203–213.
Maestre, F. T., D. A. Ramírez, and J. Cortina (2007), Ecología del esparto (*Stipa tenacissima L.*) y los espartales de la Península Ibérica, *Ecosistemas*, *16*(2), 111–130.
Maestre, F. T., et al. (2009), Shrub encroachment can reverse desertification in semi-arid Mediterranean grasslands, *Ecol. Lett.*, *12*(9), 930–941.
Marañón-Jiménez, S., J. Castro, A. S. Kowalski, P. Serrano-Ortiz, B. R. Reverter, E. P. Sánchez-Cañete, and R. Zamora (2011), Post-fire soil respiration in relation to burnt wood management in a Mediterranean mountain ecosystem, *For. Ecol. Manage.*, *261*(8), 1436–1447.
Mauder, M., and T. Foken (2006), Impact of post-field data processing on eddy covariance flux estimates and energy balance closure, *Meteorol. Z.*, *15*(6), 597–609.
Mayor, Á. G., S. Bautista, and J. Bellot (2011), Scale-dependent variation in runoff and sediment yield in a semiarid Mediterranean catchment, *J. Hydrol.*, *397*(1–2), 128–135.
Metcalfe, D. B. (2014), Climate science: A sink down under, *Nature*, *509*(7502), 566–567.
Migliavacca, M., et al. (2011), Semiempirical modeling of abiotic and biotic factors controlling ecosystem respiration across eddy covariance sites, *Global Change Biol.*, *17*(1), 390–409.
Moncrieff, J. B., J. M. Massheder, H. de Bruin, J. Elbers, T. Friborg, B. Heusinkveld, P. Kabat, S. Scott, H. Soegaard, and A. Verhoef (1997), A system to measure surface fluxes of momentum, sensible heat, water vapour and carbon dioxide, *J. Hydrol.*, *188–189*, 589–611.

Moncrieff, J., R. Clement, J. Finnigan, and T. Meyers (2005), Averaging, detrending, and filtering of eddy covariance time series, in *Handbook of Micrometeorology*, edited by X. Lee, W. Massman, and B. Law, pp. 7–31, Springer, Netherlands.
Noy-Meir, I. (1973), Desert ecosystems: Environment and producers, *Annu. Rev. Ecol. Syst.*, *4*(1), 25–51.
Okin, G. S. (2001), Wind-driven desertification: Process modeling, remote monitoring, and forecasting, PhD thesis, California Institute of Technology Pasadena, California, Pasadena, Calif.
Padilla, F. M., J. D. D. Miranda, C. Armas, and F. I. Pugnaire (2015), Effects of changes in rainfall amount and pattern on root dynamics in an arid shrubland, *J. Arid Environ.*, *114*, 49–53.
Parton, W., J. Morgan, D. Smith, S. Del Grosso, L. Prihodko, D. LeCain, R. Kelly, and S. Lutz (2012), Impact of precipitation dynamics on net ecosystem productivity, *Global Change Biol.*, *18*(3), 915–927.
Pérez-Priego, O., L. Testi, F. Orgaz, and F. J. Villalobos (2010), A large closed canopy chamber for measuring CO_2 and water vapour exchange of whole trees, *Environ. Exp. Bot.*, *68*(2), 131–138.
Pérez-Priego, O., A. López-Ballesteros, E. Sánchez-Cañete, P. Serrano-Ortiz, L. Kutzbach, F. Domingo, W. Eugster, and A. Kowalski (2015), Analysing uncertainties in the calculation of fluxes using whole-plant chambers: Random and systematic errors, *Plant Soil*, *393*(1), 229–244.
Poulter, B., et al. (2014), Contribution of semi-arid ecosystems to interannual variability of the global carbon cycle, *Nature*, *509*(7502), 600–603.
Pugnaire, F. I., and P. Haase (1996), Comparative physiology and growth of two perennial tussock grass species in a semi-arid environment, *Ann. Bot.*, *77*(1), 81–86.
Pugnaire, F. I., P. Haase, L. D. Incoll, and S. C. Clark (1996), Response of the tussock grass *Stipa tenacissima* to watering in a semi-arid environment, *Funct. Ecol.*, *10*(2), 265–274.
Ramírez, D. A. (2006), Estudio de la transpiración del esparto (*Stipa tenacissima L.*) en una cuenca del semiárido alicantino: Un análisis pluriescalar, PhD thesis, Dep. Ecology, Univ. of Alicante, Alicante, Spain.
Reichstein, M., et al. (2005), On the separation of net ecosystem exchange into assimilation and ecosystem respiration: Review and improved algorithm, *Global Change Biol.*, *11*(9), 1424–1439.
Rejos, F. J. (2000), La Atocha (*Stipa tenacissima Loefl. ex L.*) en el centro peninsular: Aspectos vegetativos y reproductivos, PhD thesis, Univ. of Alcalá, Madrid, Spain.
Rey, A., L. Belelli-Marchesini, A. Were, P. Serrano-ortiz, G. Etiope, D. Papale, F. Domingo, and E. Pegoraro (2012), Wind as a main driver of the net ecosystem carbon balance of a semiarid Mediterranean steppe in the South East of Spain, *Global Change Biol.*, *18*(2), 539–554.
Ross, I., L. Misson, S. Rambal, A. Arneth, R. L. Scott, A. Carrara, A. Cescatti, and L. Genesio (2012), How do variations in the temporal distribution of rainfall events affect ecosystem fluxes in seasonally water-limited Northern Hemisphere shrublands and forests?, *Biogeosciences*, *9*(3), 1007–1024.
Rutledge, S., D. I. Campbell, D. Baldocchi, and L. A. Schipper (2010), Photodegradation leads to increased carbon dioxide losses from terrestrial organic matter, *Global Change Biol.*, *16*(11), 3065–3074.
Rychnovská, M. (1964), A contribution to the ecology of the genus *Stipa* II. Water relations of plants and habitat on the hill Krížová hora near the town of Moravský, *Preslia (Praha)*, *37*, 42–52.
Sala, O. E., and W. K. Lauenroth (1985), Root profiles and the ecological effect of light rainshowers in arid and semiarid regions, *Am. Midl. Nat.*, *114*(2), 406–408.
Sánchez-Cañete, E. P., and A. S. Kowalski (2014), Comment on "Using the gradient method to determine soil gas flux: A review" by M. Maier and H. Schack-Kirchner, *Agric. For. Meteorol.*, *197*, 254–255.
Schlesinger, W. H. (1990), Evidence from chronosequence studies for a low carbon-storage potential of soils, *Nature*, *348*(6298), 232–234.
Schwinning, S., and O. Sala (2004), Hierarchy of responses to resource pulses in arid and semi-arid ecosystems, *Oecologia*, *141*(2), 211–220.
Scott, R. L., E. P. Hamerlynck, G. D. Jenerette, M. S. Moran, and G. A. Barron-Gafford (2010), Carbon dioxide exchange in a semidesert grassland through drought-induced vegetation change, *J. Geophys. Res.*, *115*, G03026, doi:10.1029/2010JG001348.
Scott, R. L., P. Serrano-Ortiz, F. Domingo, E. P. Hamerlynck, and A. S. Kowalski (2012), Commonalities of carbon dioxide exchange in semiarid regions with monsoon and Mediterranean climates, *J. Arid Environ.*, *84*, 71–79.
Serrano-Ortiz, P., C. Oyonarte, O. Pérez-Priego, B. Reverter, E. P. Sánchez-Cañete, A. Were, O. Uclés, L. Morillas, and F. Domingo (2014), Ecological functioning in grass–shrub Mediterranean ecosystems measured by eddy covariance, *Oecologia*, *175*(3), 1005–1017.
Solomon, S., G. K. Plattner, R. Knutti, and P. Friedlingstein (2009), Irreversible climate change due to carbon dioxide emissions, *Proc. Natl. Acad. Sci. U. S. A.*, *106*(6), 1704–1709.
Sponseller, R. A. (2007), Precipitation pulses and soil CO_2 flux in a Sonoran Desert ecosystem, *Global Change Biol.*, *13*(2), 426–436.
Thomey, M. L., S. L. Collins, R. Vargas, J. E. Johnson, R. F. Brown, D. O. Natvig, and M. T. Friggens (2011), Effect of precipitation variability on net primary production and soil respiration in a Chihuahuan Desert grassland, *Global Change Biol.*, *17*(4), 1505–1515.
Unger, S., C. Máguas, J. S. Pereira, T. S. David, and C. Werner (2010), The influence of precipitation pulses on soil respiration—Assessing the "Birch effect" by stable carbon isotopes, *Soil Biol. Biochem.*, *42*(10), 1800–1810.
Unger, S., C. Máguas, J. S. Pereira, T. S. David, and C. Werner (2012), Interpreting post-drought rewetting effects on soil and ecosystem carbon dynamics in a Mediterranean oak savannah, *Agric. For. Meteorol.*, *154-155*, 9–18.
Valladares, F., and F. I. Pugnaire (1999), Tradeoffs between irradiance capture and avoidance in semi-arid environments assessed with a crown architecture model, *Ann. Bot.*, *83*(4), 459–469.
Wagner, S. W., D. C. Reicosky, and R. S. Alessi (1997), Regression models for calculating gas fluxes measured with a closed chamber, *Agron. J.*, *89*(2), 279–284.
Webb, E. K., G. I. Pearman, and R. Leuning (1980), Correction of flux measurements for density effects due to heat and water vapour transfer, *Q. J. R. Meteorol. Soc.*, *106*(447), 85–100.
Weijermars, R. (1991), Geology and tectonics of the Betic Zone, SE Spain, *Earth Sci. Rev.*, *31*(3–4), 153–236.
Williams, C., N. Hanan, R. Scholes, and W. Kutsch (2009), Complexity in water and carbon dioxide fluxes following rain pulses in an African savanna, *Oecologia*, *161*(3), 469–480.
Wingler, A., P. J. Lea, W. P. Quick, and R. C. Leegood (2000), Photorespiration: Metabolic Pathways and Their Role in Stress Protection, *Philos. Trans. R. Soc. London, Ser. B*, 355, 1517–1529.
Wohlfahrt, G., L. F. Fenstermaker, and J. A. Arnone III (2008), Large annual net ecosystem CO_2 uptake of a Mojave Desert ecosystem, *Global Change Biol.*, *14*(7), 1475–1487.
World Reference Base for Soil Resources (2006), *World Soil Resources Reports 103*, FAO, Rome, Italy.
Xu, L., D. D. Baldocchi, and J. Tang (2004), How soil moisture, rain pulses, and growth alter the response of ecosystem respiration to temperature, *Global Biogeochem. Cycles*, *18*, GB4002, doi:10.1029/2004GB002281.
Yan, L., S. Chen, J. Huang, and G. Lin (2011), Water regulated effects of photosynthetic substrate supply on soil respiration in a semiarid steppe, *Global Change Biol.*, *17*(5), 1990–2001.
Zhang, Y., et al. (2013), Extreme precipitation patterns and reductions of terrestrial ecosystem production across biomes, *J. Geophys. Res. Biogeosci.*, *118*, 148–157, doi:10.1029/2012JG002136.